Coarse topographic organization of pheromone-sensitive afferents from different antennal surfaces in the American cockroach

Hiroshi Nishino[a]†, Hidehiro Watanabe[b]†, Itsuro Kamimura[c], Fumio Yokohari[b], Makoto Mizunami[d]

[a]Research Institute for Electronic Science, Hokkaido University, Sapporo 060-0812, Japan

[b]Faculty of Science, Fukuoka University, Fukuoka 814-0180, Japan

[c]Maxnet Co., Ltd., Tokyo 164-0001, Japan

[d]Faculty of Science, Hokkaido University, Sapporo 060-0810, Japan

The corresponding author: Hiroshi Nishino, Research Institute for Electronic Science, Hokkaido University, Sapporo 060-0812, Japan.

Tel: +81-11-706-2596

Email: nishino@es.hokudai.ac.jp

†These authors contributed equally to this work.

Abstract

In contrast to visual, auditory, taste, and mechanosensory neuropils, in which sensory afferents are topographically organized on the basis of their peripheral soma locations, axons of cognate sensory neurons from different locations of the olfactory sense organ converge onto a small spherical neuropil (glomerulus) in the first-order olfactory center. In the cockroach *Periplaneta americana*, sex pheromone-sensitive afferents with somata in the antero-dorsal and postero-ventral surfaces of a long whip-like antenna are biased toward the anterior and posterior regions of a macroglomerulus, respectively. In each region, afferents with somata in the more proximal antenna project to more proximal region, relative to the axonal entry points. However, precise topography of afferents in the macroglomerulus has remained unknown. Using single and multiple neuronal stainings, we showed that afferents arising from anterior, dorsal, ventral and posterior surfaces of the proximal regions of an antenna were biased progressively from the anterior to posterior region of the macroglomerulus, reflecting chiasmatic axonal re-arrangements that occur immediately before entering the antennal lobe. Morphologies of individual afferents originating from the proximal antenna matched results of mass neuronal stainings, but their three-dimensional origins in the antenna were hardly predictable on the basis of the projection patterns. Such projection biases made by neuronal populations differ from strict somatotopic projections of antennal mechanosensory neurons in the same species, suggesting a unique sensory mechanism to process information about odor location and direction on a single antenna.

Keywords: insects; olfactory afferents; glomerulus; topographic map; sex pheromone; antenna

Accurate representation of the stimulus source is fundamental in sensory processing. The key neuroanatomical feature is the topographic sensory map seen in the central nervous system, where axon terminals are organized on the basis of cellular arrangements in the peripheral sense organ [1]. This topographic map, therefore, allows animals to localize the stimulus source, discriminate stimuli of different locations, and further reconstruct the object shape by integrating multiple stimulus sources. The most well-known examples are the "homunculus" in the somatosensory cortex of humans, in which peripheral arrangements of mechanosensory neurons from different body regions are conserved in the brain [1]. A similar topographic organization of afferents is also seen in the visual, taste, and auditory systems [1].

In contrast, cognate sensory neurons, generally scattered throughout the olfactory epithelium, converge axons onto a small spherical neuropilar unit, the glomerulus [2]. Each glomerulus consists of a large number of incoming sensory afferents and dendrites of a smaller number of second-order (projection) neurons and local interneurons [2]. This unique glomerular organization is important for detecting and differentiating minute quantities of volatile chemicals [3,4]. On the other hand, several studies have shown that odor plumes emitted from an odor source are not smooth and continuous with a clear concentration gradient but, rather, are composed of filaments of various sizes (> mm) and concentrations interspersed with regions of clean air, suggesting that fine-scale topographic structures exist within odor plumes [5,6].

We have found that an elaborate topographic organization of sensory afferents exists in the sex pheromone-receptive macroglomerulus (B-glomerulus) of the American cockroach [7]. The B-glomerulus is the largest in the male antennal lobe and is specialized for processing periplanone-B (a major pheromone component) [8]. Periplanone-B is especially important for attracting conspecific males from long distances [9]. The B-glomerulus receives convergent projections from single sensory neurons housed by approximately 36,000 *single-walled* B (*s-w* B*)* sensilla distributed throughout the antennal flagellum (the third antennal segment) [10,11]. Firstly, afferents arising from the sensilla on the antero-dorsal half surface of the flagellum and those on the postero-ventral half surface of the flagellum are biased toward the anterior half and the posterior half of the B-glomerulus [7]. A similar topographic organization of afferents based on anterior and posterior surfaces of the flagellum has been detected in pheromone-sensitive glomeruli of several moth species [12-14]. Secondly, afferents

arising from sensilla on the more proximal region of the flagellum tend to project progressively to the more proximal region of the glomerulus, relative to axonal entry points [7]. According to these features, three-dimensional locations of pheromone-sensitive neurons are roughly mapped in the B-glomerulus.

Now the question arises as to how precisely this topographic sensory map represents the stimulus location. So far, no attempts have been made to characterize projection patterns of cognate olfactory sensory neurons arising from different antennal surfaces in any insects. We used nerve section stainings and single sensillum stainings and evaluated the topography of sensory afferents in the B-glomerulus.

Adult male cockroaches (*Periplaneta americana*) with intact antennae (Fig. 1a), reared in a 12:12-hour light–dark cycle at 27 ˚C, were used. The anterior and posterior nerves, two parallel antennal nerves, contain sensory axons arising from various types of sensilla on the flagellar surface (Fig. 1b-d). Three sets of anterograde stainings of sensory neuronal axons were achieved as follows: 1) differential stainings of a bisection of each antennal nerve, 2) stainings of a small section of each nerve, and 3) single sensillum stainings. The dissection procedures were the same as those in our previous studies [7,11]. In the first experiment, either of the two nerves was split into bisection by an electrolytically tapered tungsten rod and cut with microscissors at the fifth flagellar annulus; their distal cut-ends were then placed separately into two tapered glass electrodes containing either 10% microruby (D-7162, Invitrogen, USA) or 10% microemerald (D-7156, Invitrogen, USA). The preparation was incubated in a humid chamber at 5 ˚C for 48 h for diffusion of the dye. In the second experiment, about a 1/4 section of axonal bundles was separated from each nerve and the cut-end was immersed in a low molecular weight dye (6% nickel chloride hexahydrate). The preparation was incubated in a humid chamber at 5˚C up to 36 h. The specimens were subsequently intensified with silver [15]. In the third experiment, the *sw-B* sensillum was clipped and then covered with an electrode containing 10% microruby (Fig. 1e). The preparation was incubated at 10 ˚C for 2 days and consecutively at 4 ˚C for 2 days in a humid chamber (see [11] for details).

After the incubation, the brain and the antenna were dissected free from the head capsule, fixed in a 4% formaldehyde solution, dehydrated in an ascending ethanol series, and then cleared in methyl salicylate. The cleared brain and the antenna were viewed anteriorly using a confocal laser-scanning microscope, LSM 5 Pascal or LSM 510 (Carl

Zeiss, Jena, Germany). The three-dimensional location of a sensillum was identified using hair plates on the pedicel as landmarks and its axons were traced by removing part of the cuticle (Fig. 1f and g). Afferents labeled by microemerald were visualized by confocal microscopy using an argon laser (Lasos Lasertechnik GmbH, Jena, Germany) with a band-pass filter (505–530 nm), whereas those labeled by microruby were visualized using a helium–neon laser (Lasos Lasertechnik GmbH) with a long-pass filter (560 nm). The outline of the B-glomerulus was imaged by autofluorescence using the argon laser. Optical sections made at 1.0–1.2 μm were reconstructed three-dimensionally with Amira 5.33 software (Mercury Computer Systems, Berlin, Germany).

For quantitative analysis, tips of afferent terminals derived from different individuals were detected by the "seeded region growing" and "skeletonized" functions in Amira. The shortest distances between afferent tips and the lateral margin of the B-glomerulus outline were calculated using Microsoft Excel 2010. After the coordinated values derived from different individuals had been normalized according to the longitudinal length of the B-glomerulus, the distances, the locations along the lateral edge of the glomerular outline, and the locations along the anterior-posterior axis were plotted on X, Y, and Z axes in three-dimensional plots using Amira (see Fig. 3o). The cross-sectional area of axons immediately before entering the B-glomerulus was measured by Amira. Observations of the surface structure of the antenna were made with a scanning electron microscope (S-4800; Hitachi, Tokyo, Japan). The body axis was used as the reference against which position and direction were defined.

The antennal flagellum of the cockroach is composed of repeating segments called annuli, and it tapers distally, its diameter being approximately 400 μm in the most proximal region and 130 μm in the most distal region (Fig. 1a). Each *s-w* B sensillum generally houses four sensory neurons, two of which are sensitive to periplanone-A (a minor sex pheromone component) and periplanone-B, respectively, and the other two of which are sensitive to other monoteropenoid odors. [16]. Sensory neurons arising from sensilla on the antero-dorsal half surface (magenta) and the postero-ventral half surface of the flagellum (green) send axons to the anterior and posterior nerves, respectively [7] (Fig. 1c and d). Axons of sensory neurons from the *s-w* B sensillum form a thin nerve bundle together with axons from nearby olfactory, mechano and contact-chemo sensilla, which joins in the peripheral region of the primary nerve (Fig. 1g).

Differential anterograde stainings of a bisection of each nerve revealed detailed axonal entry patterns into the B-glomerulus. The anterior and posterior nerves crossed at the base of the antenna (blue arrow, Fig. 1b) so that axons arising from the anterior, dorsal, ventral and posterior antennal surfaces (Fig. 2o and p) were re-arranged from antero-ventral to postero-dorsal (Fig. 2q). Due to the close apposition of the B-glomerulus to the antennal nerves (Fig. 2 a and b), axonal bundles diverging from the anterior, dorsal, ventral and posterior nerve sections tended to progressively enter from ventral to lateral along the anterior-posterior axis of the glomerulus (Fig. 2c-j and Supplementary data file A).

The axonal entries along the antero-posterior axis of the B-glomerulus were reflected in the distribution of afferents within the B-glomerulus. Afferents arising from each of the four antennal surfaces were distributed throughout the B-glomerulus (Supplementary data files B and C), but the relative amounts of them differed along the anterior-posterior axis (Fig. 2r). Afferents arising from the anterior surface (green) and dorsal surface (magenta) were predominantly seen in the anteriormost and anterior-central regions of the B-glomerulus (Fig. 2c-f; n=6), while those arising from the ventral surface (magenta) and the posterior surface (green) were more predominantly seen in the posterior-central and posteriormost regions (Fig. 2g-j; n=6). Small nerve section stainings using heavy metal and subsequent intensification revealed that axons from the anteriormost, dorsalmost, ventralmost, and posteriormost antennal surfaces anticlockwisely entered antero-ventrally to postero-laterally and their afferents were more profusely distributed in the same anterior-posterior focal plane (Fig. 2k-n). These results were in good agreement with those of fluorescent-dye labelings.

Next, we performed single sensillum stainings to evaluate axonal projection patterns of individual neurons (Fig. 3a and b). It was found that 82% of the stained afferents diverged into several axons after entering the antennal lobe, providing multiple axonal entry points at the B-glomerulus (red arrows, Fig. 3c-f, h, i, k, l and n; Supplementary data file D). Individual afferents showed diverse morphologies. Most of the stained afferents had localized branches (Fig. 3e-h, j, and k) or those with a few collaterals (Fig. 3d,l, and m). A few afferents had rather dispersed branches (Fig. 3c,i and n). Branches of each afferent tended to be more abundant close to the axonal entry points (Fig. 3c-n). Accordingly, three-dimensional plots of the terminal tips of 22 afferents in the normalized B-glomerulus revealed that presumed varicosities of afferents from the

antero-dorsal surface (reddish) and postero-ventral surface (greenish) of proximal annuli are biased toward the antero-ventral and postero-lateral regions of the B-glomerulus, respectively (Fig. 3p and q; Supplementary data file E). However, sensilla arising from similar three-dimensional locations but from different individuals tended to have distinct branching patterns (Fig. 3i-k). Thus, at the single neuronal level, three-dimensional origins of somata on the circumference of the flagellum were not predictable based solely on projection profiles.

We observed that sex pheromone-sensitive afferents arising from the four surfaces of the antenna exhibit biased distributions in the B-glomerulus, creating projection waves along its anterior-posterior axis. Such projection profiles were blurred at single sensory neurons due to their varied morphologies and individual variation. This was in contrast to antennal mechanosensory projections in the same species, in which sensory neurons on different circumferences of the flagellum project to different sets of neuropilar layers in the deutocerebrum [17].

Although morphologies of single neuronal afferents were too diverse to characterize unique projection patterns based on three-dimensional origins, the possibility that finer projection biases based on different antennal surfaces exist can not be ruled out. Obtaining more samples, ideally with differential labelings of two closely located sensilla in the same individual, is necessary to evaluate this possibility.

It is tempting to speculate that the coarse topographic organization of olfactory afferents is an evolutional trade-off to enable both amplification of weak stimuli [3] and topographical representation of stimuli, because more localized projections of individual afferents result in lower convergence rates on the input sites of dendrites of projection neurons, losing the structural advantage as a “glomerulus”. Some arthropod-specific features may promote detection of spatial odor distribution in early odor processing. For example, insect odor receptors have been suggested to be ligand-gated ion channels [18], allowing faster (i.e., biologically more meaningful) representation of odor distribution, than that by vertebrate G protein-coupled receptors [19]. If the flicking cockroach antenna has a fluid filtering system comparable to the lobster antennule [20], odor retention in sensilla on a particular antennal surface could be facilitated, because the fluid in contact with the surface of a moving object does not slip relative to the object and a velocity gradient develops in the flow around the object [20].

The two organizational rules of afferents may be related to topographic odor representation in projection neurons. Firstly, according to the developmental rule that newly emerged olfactory afferents arising from the proximal annuli are added to the pre-existing glomerulus [21], afferents arising from proximal annuli tended to have more branches close to the axonal entry points. Therefore, afferents from the proximal (thicker) region of the flagellum are more broadly distributed along the anterior-posterior axis of the glomerulus than are those from the distal (thinner) region, possibly facilitating discrimination of odors on different antennal surfaces by projection neurons in the proximal antenna. Secondly, afferents from the anterior/posterior surfaces were spatially more segregated than were those from dorsal/ventral surfaces of the flagellum in the B-glomerulus. This may be related to the directional preference of odors across the longitudinal antenna. Neurophysiological and ultrastructural studies are needed to understand how the topography of afferents is exploited by projection neurons.

Acknowledgments

This work was supported by a grant from the Ministry of Education, Science, Technology, Sports and Culture of Japan to H.N. (Grant number: 26440175).

References

[1] E.R. Kandel, J.H. Schwartz, T.M. Jessell, S. Siegelbaum, A.J. Hudspeth, Principles of Neural Science, Fifth edition (2012).

[2] L.M. Kay, M. Stopfer, Information processing in the olfactory systems of insects and vertebrates. Semin. Cell Dev. Biol. 17 (2006) 433-442.

[3] R. Tabuchi, T. Sakurai, H. Mitsuno, S. Namiki, R. Minegishi, T. Shiotsuki, K. Uchino, H. Sezutsu, T. Tamura, S.S. Haupt, K. Nakatani, R. Kanzaki, Pheromone responsiveness threshold depends on temporal integration by antennal lobe projection neurons. Proc. Nat. Acad. Sci USA 110 (2013) 15455–15460.

[4] R. Wilson Early olfactory processing in *Drosophila*: mechanisms and principles. Ann. Rev. Neurosci. 36 (2013) 217-241.

[5] J.P. Crimaldi, J.R. Koseff, High-resolution measurements of the spatial and temporal scalar structure of a turbulent plume. Experiments in Fluid 31 (2001) 90-102.

[6] R.T. Carde, M.A. Willis, Navigational strategies used by insects to find distant, wind-borne sources of odor. J. Chem. Ecol. 34 (2008) 854-866.

[7] H. Nishino, M. Mizunami, Sensilla position on antennae influences afferent terminal location in glomeruli. NeuroReport 18 (2007) 1765-1769.

[8] M. Burrows, J. Boeckh, J. Esslen, Physiological and morphological properties of interneurons in the deutocerebrum of male cockroaches which respond to female pheromone. J. Comp. Physiol. 145 (1982) 447-457.

[9] G. Seelinger, Behavioural responses to female sex pheromone components in *Periplaneta americana*. Anim. Behav. 33 (1985) 591–598.

[10] D. Schaller, Antennal sensory system of *Periplaneta americana* L. Distribution and

frequency of morphologic types of sensilla and their sex-specific changes during postembryonic development. Cell Tissue Res. 191 (1978) 121-139.

[11] H. Watanabe, S.S. Haupt, H. Nishino, M. Nishikawa, F. Yokohari, Sensilla-specific, topographic projection patterns of olfactory receptor neurons in the antennal lobe of the cockroach *Periplaneta americana*. J. Comp. Neurol. 520 (2012) 1687-1701.

[12] T.A. Christensen, I.D. Harrow, C. Cuzzocrea, P. Randolph, J.G. Hildebrand, Distinct projections of two populations of olfactory receptor axons in the antennal lobe of the sphinx moth *Manduca sexta*. Chem. Senses 20 (1994) 313–323.

[13] H. Ai, R. Kanzaki, Modular organization of the silkmoth antennal lobe macroglomerular complex revealed by voltatge-sensitive dye imaging. J. Exp. Biol. 207 (2004) 633–644.

[14] B.G. Berg, T.J. Almaas, J.G. Bjaalie, H. Mustaparta, Projections of male-specific receptor neurons in the antennal lobe of the oriental tobacco budworm moth, *Helicoverpa assulta*: a unique glomerular organization among related species. J. Comp. Neurol. 486 (2005) 209 –220.

[15] J.P. Bacon, J.S. Altman, A silver intensification method for cobalt-filled neurons in wholemount preparations. Brain Res. 138 (1977) 359–363.

[16] H. Sass, Production, release and effectiveness of two female sex pheromone components of *Periplaneta americana*. J. Comp. Physiol. 152 (1983) 309-317.

[17] H. Nishino, M. Nishikawa, F. Yokohari, M. Mizunami, Dual, multi-layered somatosensory maps formed by antennal tactile and contact chemosensory afferents in an insect brain. J. Comp. Neurol. 493 (2005) 291–308.

[18] K. Sato, M. Pellegrino, T. Nakagawa, T. Nakagawa, L.B. Vosshall, K. Touhara, Insect olfactory receptors are heteromeric ligand-gated ion channels. Nature 452 (2008)

1002-1006.

[19] U.B. Kaupp, Olfactory signaling in vertebrates and insects: differences and commonalities. Nat. Rev. Neurosci. 11 (2010) 188-200.

[20] M.A.R. Koehl, J.R. Koseff, J.P. Crimaldi, M.G. McCay, T. Cooper, M. B. Wiley, P.A. Moore, Lobster sniffng: antennule design and hydrodynamic filtering of information in an odor plume. Science 294 (2001) 1948-1951.

[21] H. Nishino, A. Yoritsune, M. Mizunami, Different growth patterns of two adjacent glomeruli responsible for sex-pheromone processing during postembryonic development of the cockroach *Periplaneta americana.* Neurosci. Lett. 462 (2009) 219-224.

Figure Legends

Fig. 1. Two parallel antennal nerves in the antennal flagellum. (a) Semi-schematic diagram of the tapered antenna segmented into more than 140 annuli. (b) Proximal region of the flagellum, showing chiasmatic re-arrangements of two antennal nerves (blue arrow). (c) Two antennal nerves running in parallel in the 26-29 annuli. (d) Cross section of the flagellum at the 1st annulus, showing two equal-sized antennal nerves attached to the inside of the antennal cuticle. Note slight shrinkage of the nerve due to the fixation process. (e) An electrode filled with microruby covering a single sensillum. (f) Single *s-w* B sensillum on the 11th annulus marked by microruby (magenta). (g) A single axon from a single sensillum on the 4th annulus runs in the periphery of the posterior nerve. Scale bars = 5 mm in (a), 1 mm in (b), 100 μm in (c,d), 50 μm in (e-g).

Fig. 2. Projection patterns of antennal nerve sections, viewed anteriorly (a-n) and laterally (o-r). (a and b) Antennal lobes in which bisections of the anterior nerve (a) and posterior nerve (b) were differentially stained. (c-j) Confocal stacks at different antero-posterior regions showing afferents from anterior (green), dorsal (magenta), ventral (magenta) and posterior (green) surfaces are biased toward the anterior-most,

antero-central, postero-central, and posteriormost regions of the B-glomerulus, reflecting axonal entries (white arrows). Sensory tracts (T I- T IV) progressively enter from antero-ventral to posterior-lateral of the B-glomerulus (see Supplementary data file A for details). Numbers indicate distances from the anterior margin of the B-glomerulus. (k-h) About 1/4 nerve section stainings and subsequent silver intensification, showing anticlockwise axon entries (red arrows) from ventral to lateral along the antero-posterior axis of the B-glomerulus. (o-r) Schematic representation of antennal nerve topography (p), chiasmatic nerve crossing (q), and afferents in the B-glomerulus (r) viewed laterally (o). Scale bars = 100 μm in (a,b and k-n), 50 μm in (c-j), 1 mm in (o).

Fig. 3. Single sensory afferents innervating the B-glomerulus. (a and b) Locations of individual sensilla stained in the flagellum. (c-n) Axon terminals of single afferents from the antero-dorsal half (c-h) and the postero-ventral half surfaces (i-n) of the flagellum, viewed anteriorly (upper column) and dorsally (lower column). Red arrows indicate axonal entries to the B-glomerulus (green). (o-q) 3D mapping procedures of tips of afferents in the normalized B-glomerulus (o) showing distribution patterns of 22 afferents viewed anteriorly (p) and dorsally (q). Presumed varicosities of different afferents belonging to the antero-dorsal surface (reddish) and postero-ventral surface (greenish) are generally segregated. Different shapes and color density represent different afferents (See supplementary figure D). Scale bars = 500 μm in (a,b) and 50 μm in (c-n and o).

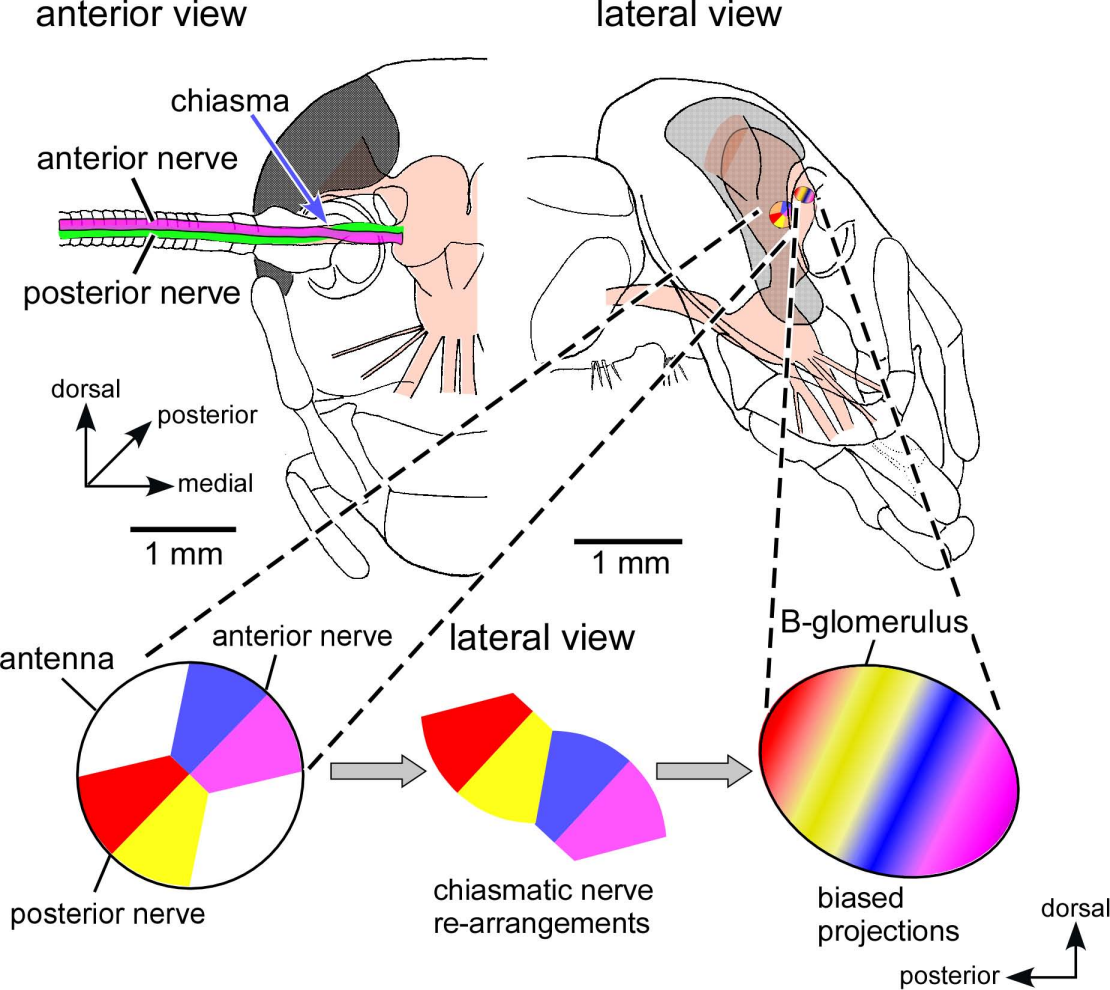
anterior view
lateral view
chiasma
anterior nerve
posterior nerve
dorsal
posterior
medial
1 mm
1 mm
antenna
anterior nerve
lateral view
B-glomerulus
posterior nerve
chiasmatic nerve
re-arrangements
biased
projections
dorsal
posterior

Highlights

- Pheromone-sensitive axons from different antennal surfaces show biased projections.
- Pheromone-sensitive axons undergo chiasmatic rearrangements.
- Axonal entry patterns are reflected in biased afferent projections.
- Afferents from anterior/posterior antennal surfaces are spatially segregated.

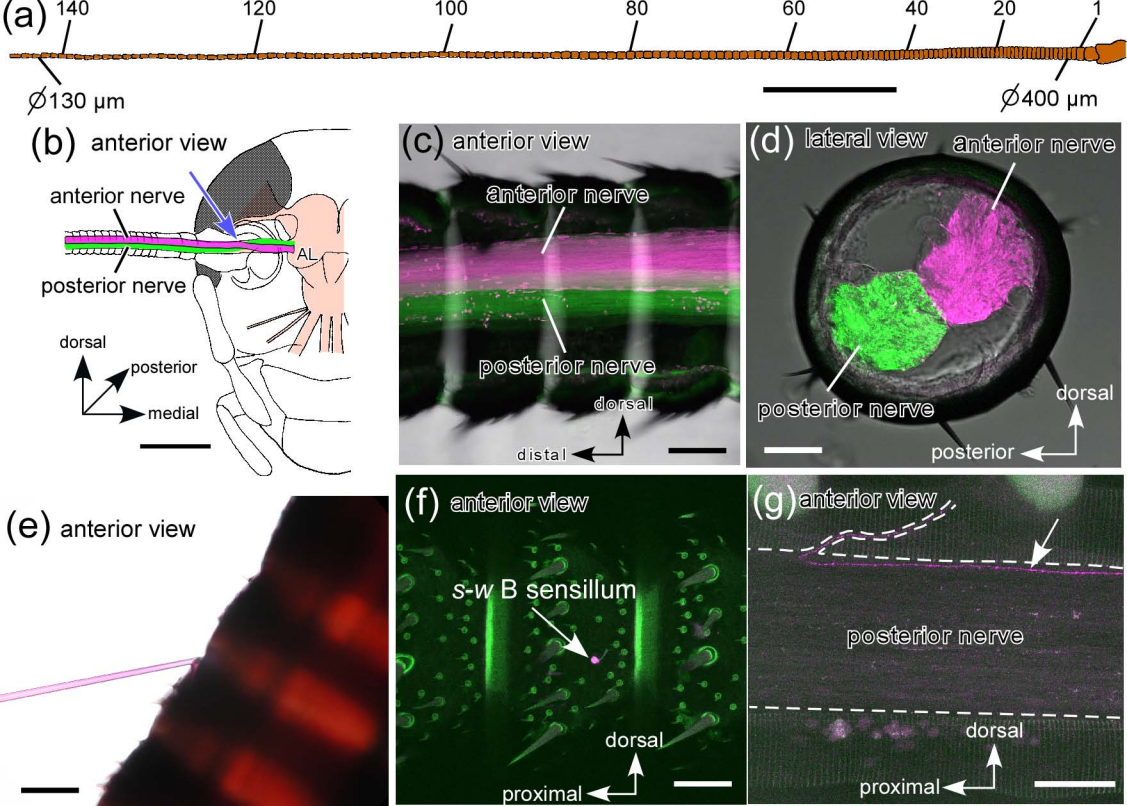
(a)
140
120
100
80
60
40
20
1
∅130 µm
∅400 µm
(b) anterior view
anterior nerve
AL
posterior nerve
dorsal
posterior
medial
(c) anterior view
anterior nerve
posterior nerve
dorsal
distal
(d) lateral view
anterior nerve
posterior nerve
dorsal
posterior
(e) anterior view
(f) anterior view
s-w B sensillum
dorsal
proximal
(g) anterior view
posterior nerve
dorsal
proximal

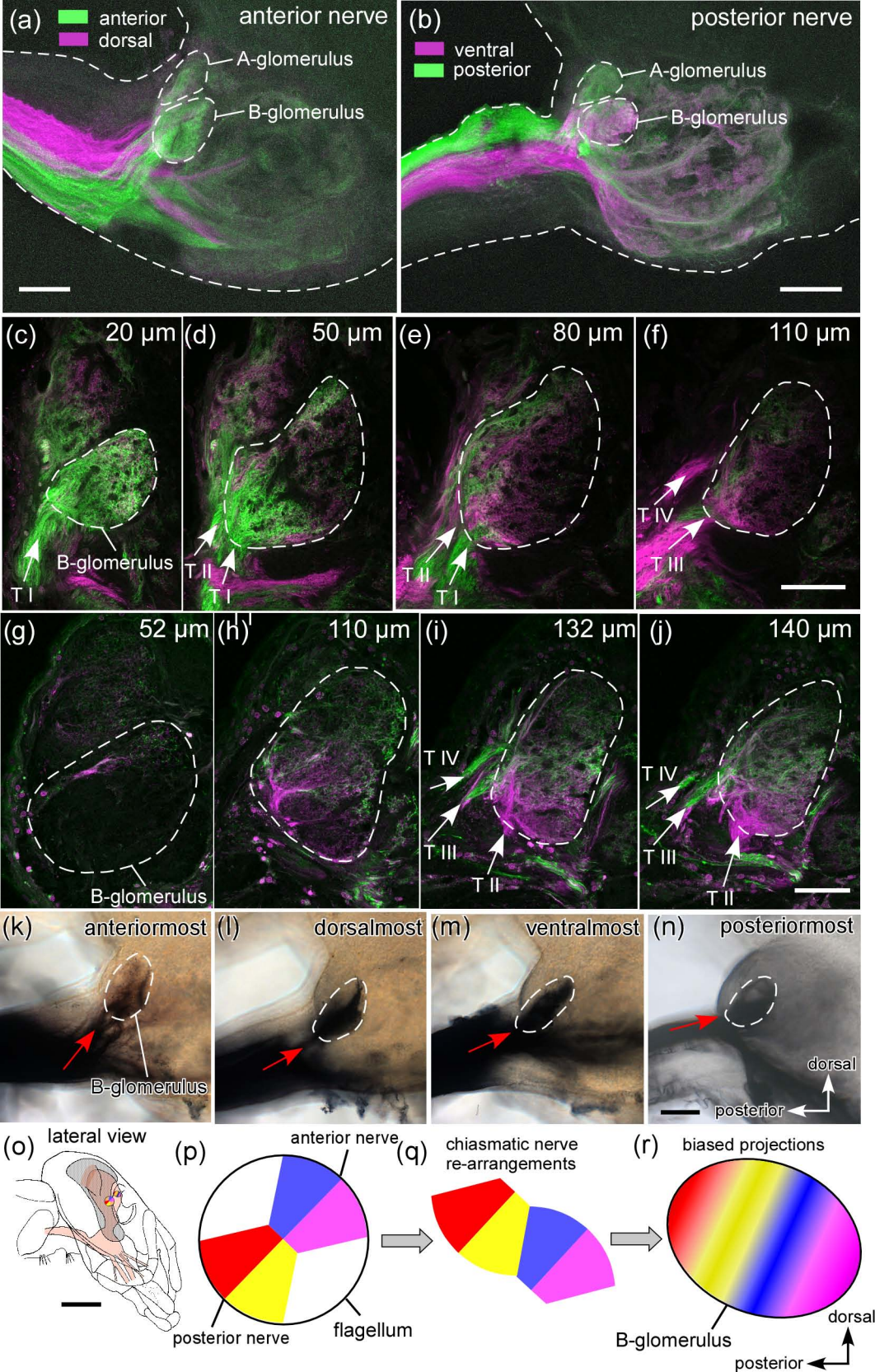
(a)
anterior
dorsal
anterior nerve
A-glomerulus
B-glomerulus
(b)
posterior nerve
ventral
posterior
A-glomerulus
B-glomerulus
(c)
20 µm
B-glomerulus
T I
(d)
50 µm
T II
T I
(e)
80 µm
T II
T I
(f)
110 µm
T IV
T III
(g)
52 µm
B-glomerulus
(h)
110 µm
(i)
132 µm
T IV
T III
T II
(j)
140 µm
T IV
T III
T II
(k)
anteriormost
B-glomerulus
(l)
dorsalmost
(m)
ventralmost
(n)
posteriormost
dorsal
posterior
(o)
lateral view
(p)
anterior nerve
posterior nerve
flagellum
(q)
chiasmatic nerve
re-arrangements
(r)
biased projections
B-glomerulus
dorsal
posterior

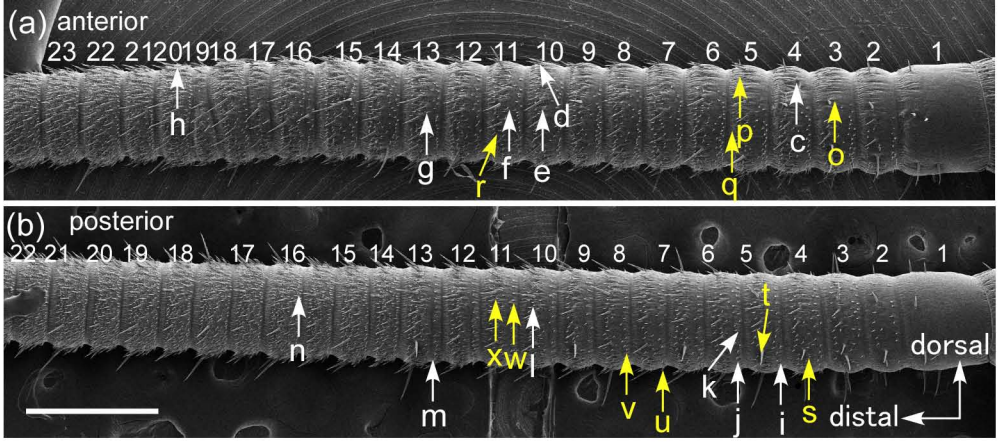

antero-dorsal surface (upper: anterior view; lower: dorsal view)

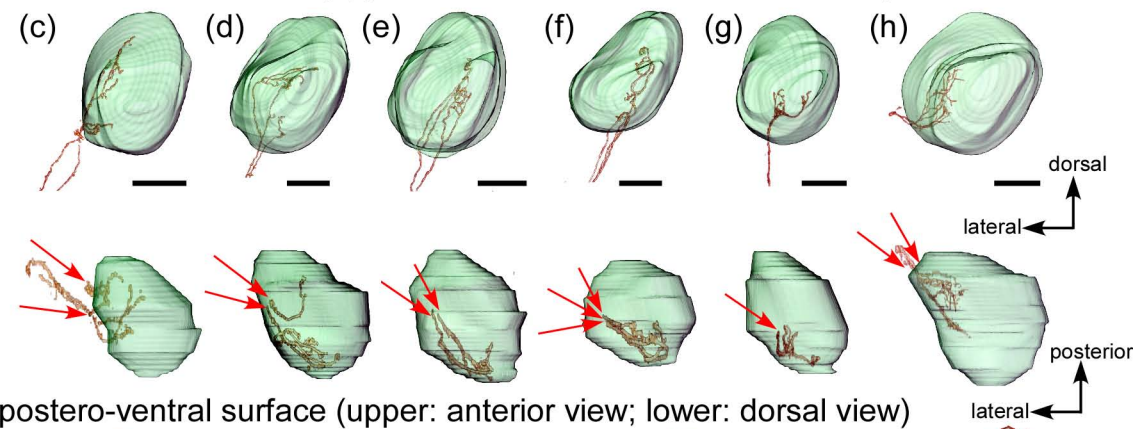

postero-ventral surface (upper: anterior view; lower: dorsal view)